The Brown Dwarf-Exoplanet Connection

Adam J. Burgasser

Massachusetts Institute of Technology

Abstract. Brown dwarfs are commonly regarded as easily-observed templates for exoplanet studies, with comparable masses, physical sizes and atmospheric properties. There is indeed considerable overlap in the photospheric temperatures of the coldest brown dwarfs (spectral classes L and T) and the hottest exoplanets. However, the properties and processes associated with brown dwarf and exoplanet atmospheres can differ significantly in detail; photospheric gas pressures, elemental abundance variations, processes associated with external driving sources, and evolutionary effects are all pertinent examples. In this contribution, I review some of the basic theoretical and empirical properties of the currently known population of brown dwarfs, and detail the similarities and differences between their visible atmospheres and those of extrasolar planets. I conclude with some specific results from brown dwarf studies that may prove relevant in future exoplanet observations.

1. A Brown Dwarf Primer

Brown dwarfs are stellar objects with insufficient mass to sustain core hydrogen fusion reactions, resulting in a steady decline in both luminosity and effective temperature (T_{eff}) with time. The mass limit for sustained hydrogen fusion is roughly 0.072 $\rm M_{\odot}$ (75 Jupiter masses) for a Solar metallicity gas mixture, increasing to 0.090 M_{\odot} for a pure hydrogen gas (e.g., Chabrier & Baraffe 2000). This mass limit establishes a formal division between "stars" and "brown dwarfs", although such a division is not necessarily relevant to how these objects form. While there is ongoing debate over the details of brown dwarf formation (the roles of gas turbulence, fragmentation and dynamical interactions; see recent reviews by Luhman et al. 2007 and Whitworth et al. 2007), observational evidence indicates brown dwarfs are created in a manner similar to, or at least coincident with, stars, via gravitational collapse of dense cores within giant molecular clouds. As a brown dwarf's energy reservoir arises primarily from the gravitational potential energy released in their initial contraction, ¹ the luminosity, T_{eff} and emergent spectral energy distribution of a brown dwarf depend primarily on mass and age, and secondarily on elemental abundances, bulk properties (e.g., rotation) and external drivers (e.g., the presence of close companion). The interdependence of these factors on brown dwarf observables

 $^{^{1}}$ Small contributions also arise from brief periods of lithium- and deuterium fusion for objects more massive than $\sim 0.065~M_{\odot}$ and $\sim 0.012~M_{\odot}$, respectively. The latter limit is considered a possible dividing line between "brown dwarfs" and "planets" (see Basri & Brown 2006), an issue that will not be touched upon here.

challenges the characterization of individual sources in the well-mixed Galactic population; however, it also provides an opportunity to study a broad range of low-temperature atmospheric properties and processes.

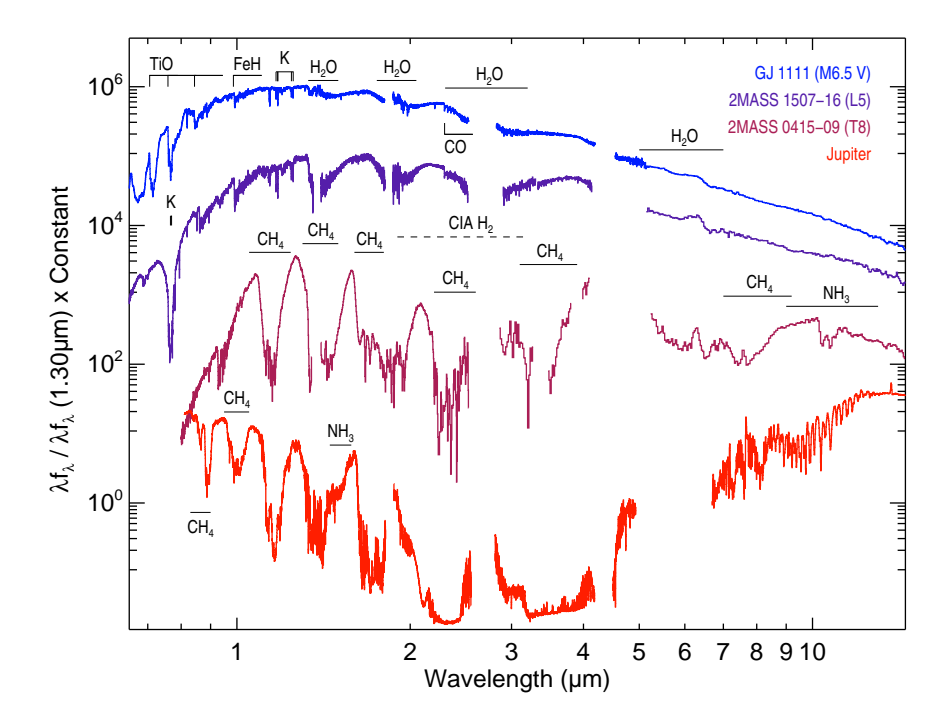


Figure 1. Observed optical to mid-infrared (0.65–14.5 μ m) spectra of representative M-type, L-type, and T-type dwarfs, compared to data for Jupiter (top to bottom). Dwarf spectra are from Cushing et al. (2006) and references therein; Jupiter data are from Rayner et al. (2009) and Kunde et al. (2004). Spectra are arbitrarily normalized. Major molecular absorption bands characterizing these spectra are labeled, including TiO, FeH, H₂, H₂O, CO, CH₄ and NH₃. Atomic K I absorption is also labeled, which produces a substantial pressure-broadened line feature spanning 0.7–0.85 μ m in L and T dwarf spectra. Note that Jupiter's emission shortward of \sim 4 μ m is dominated by scattered solar light modulated by CH₄ and NH₃ absorption features, while the dwarf spectra are entirely emergent flux (from Marley & Leggett 2008).

Brown dwarfs have been directly observed since the mid-1990s,² and there are now hundreds known to exist in young clusters, as companions to nearby stars, and, most commonly, as faint isolated systems within a few hundred parsecs of the Sun. The currently known population is segregated into three spectral classes based on the morphology of their optical or near-infrared spectra: M dwarfs, L dwarfs and T dwarfs (Figure 1). M dwarfs encompass the warmest,

²On a historical note, both the discovery of the first widely-accepted brown dwarf, Gliese 229B (Nakajima et al. 1995), and the discovery of the first extrasolar gas giant planet, 51 Peg b (Mayor & Queloz 1995), were announced to the community in the same conference, Cool Stars 9, in October 1995; see Oppenheimer et al. (2000) for a historical review.

youngest, and most massive brown dwarfs which have had little time to cool. They exhibit spectral traits similar to older, low-mass dwarf stars, with strong metal-oxide molecular bands (including TiO, VO, CO and H₂O) and neutral atomic line absorption blanketing their emergent spectral energy distributions. L dwarf spectra are characterized by strong metal-hydride (FeH, CrH), H₂O and CO molecular absorption; and alkali lines, including the heavily pressurebroadened Na I and K I doublets that largely sculpt the optical spectra of these sources (e.g., Allard et al. 2003; Burrows & Volobuyev 2003). L dwarfs also show evidence of condensate clouds in their photospheres, which give rise to highly reddened spectral energy distributions and absorption features from silicate grains (Cushing et al. 2006; see §3.1). T dwarfs are the coldest class of brown dwarfs currently known, characterized by H₂O, CH₄, NH₃ and strong collision-induced H₂ absorption. T dwarfs do not appear to have abundant condensate material in their photospheres. A fourth spectral class, the Y dwarfs, has been proposed for brown dwarfs even cooler than class T, although there is as yet no consensus on the general properties of this class nor a widely-accepted prototype (see Delorme et al. 2008; Burningham et al. 2008). The M, L and T spectral classes coincide roughly with T_{eff} ranges of $\gtrsim 2400$ K, $2400 \lesssim T_{eff} \lesssim 1400$, and $1400 \lesssim T_{eff} \lesssim 600$, respectively (Golimowski et al. 2004; Vrba et al. 2004), although the end-point of the T spectral class remains uncertain. Variations in secondary parameters, such as metallicity, age and cloud properties modulate this temperature scale (e.g., Burgasser et al. 2006; Metchev & Hillenbrand 2006; Burgasser et al. 2008). For more information on the L and T spectral classes, see the recent review of Kirkpatrick (2005).

Molecules are a prominent feature of brown dwarf atmospheres and are fundamental in our ability to ascertain the physical properties of individual sources. Beyond spectral classification, the presence, relative strengths and detailed shapes of molecular features observed in brown dwarf spectra enable measures of T_{eff} , surface gravity, metallicity, cloud composition, atmospheric dynamics, rotation, and even the presence of unseen companions (e.g., Luhman 1999; Burgasser et al. 2006; Saumon et al. 2006; Burgasser et al. 2008; Cushing et al. 2008; Reiners & Basri 2008). Extracting these details for individual brown dwarfs is a current topic of interest in the field, and a challenge due to persistent inadequacies in theoretical spectral models and opacity line lists. The complex opacities of warm molecular gases and strongly pressure-broadened atomic features (e.g., Freedman et al. 2008; also see contribution by Tennyson), dynamical effects on gas chemistry (e.g., Griffith & Yelle 1999), and the complex processes associated with condensate grain formation (e.g., Ackerman & Marley 2001; Helling & Woitke 2006) are major hurdles in bringing atmospheric models into detailed agreement with observational data. Progress is being made on the theoretical front through new work on grain formation (e.g. Helling et al. 2008; see contributions by Allard and Freytag), quantum opacity calculations for key molecules (e.g., Barber et al. 2006), and incorporation of nonequilibrium chemistry (e.g., Saumon et al. 2006; see contribution by Homeier). On the observational side, the identification of benchmark sources—companions to age-dated stars, coeval cluster members, and resolved astrometric and eclipsing binaries—are a priority as critical tests of advanced models (e.g., Mohanty et al. 2004b; Zapatero Osorio et al. 2004; Leggett et al. 2008; Dupuy et al. 2008).

2. Comparing Exoplanets to Brown Dwarfs

The benefit of brown dwarfs to exoplanet studies lies in our current ability to study their atmospheres in considerable detail, over a broad range of wavelengths and spectral resolutions, and over time. Yet for brown dwarfs to be used as reliable templates for exoplanetary studies, it is essential to first assess whether their emergent spectra faithfully guide our interpretations of emergent/reflectance planetary spectra. To this end, I examine some of key similarities and differences in the physical properties and processes of brown dwarf and exoplanet atmospheres.

2.1. Temperatures

A gross assessment of the photospheric temperatures of brown dwarfs can be inferred from their T_{eff} s. These are typically determined from bolometric luminosity measurements and an assumed (theoretical) radius estimate (e.g., Golimowski et al. 2004; Vrba et al. 2004); alternately, fits of spectral data to theoretical models are used (e.g., Mohanty et al. 2004a; Burgasser et al. 2006; Cushing et al. 2008). These measures do not always agree (Smith et al. 2003). For planets, a comparable statistic is the thermal equilibrium temperature, T_{eq} $= T_*(R_*/2a)^{1/2}$, where T_* and R_* are the effective temperature and radius of the host star, respectively, and a the semi-major axis (ignoring albedo and orbital eccentricity). As it turns out, the T_{eff} s of L- and T-type brown dwarfs overlap considerably with the T_{eq} s of transiting extrasolar planets (Figure 2). Similarly, the directly-imaged planets HR 8799bcd (Marois et al. 2008), Fomalhaut b (Kalas et al. 2008) and β Pictoris b (Lagrange et al. 2008) have estimated T_{eff} s (not T_{eg} s; see below) comparable to T dwarfs. Fomalhaut b may in fact be cooler than the $T_{eff} = 575\pm25$ K ULAS 1335, the coldest brown dwarf currently known (Burningham et al. 2008).

Transiting planets are warm due to the radiative forcing by their host stars. A planet with $T_{eq} = 500$ K lies only 0.3 AU (0.07 AU) from a solar-type (M0 dwarf) primary. As $T_{eq} \propto T_* a^{-1/2}$, more widely-orbiting planets and planets orbiting less luminous host stars have lower T_{eq} s, below the range currently sampled by brown dwarfs. For closely-orbiting, tidally-locked hot Jupiter planets, care must be taken when using T_{eq} as a proxy for photospheric temperature, as these planets can have substantial day/night asymmetries (see contribution by Knutson). Eccentricity effects can also give rise to large temporal modulations in T_{eq} (see contributions by Iro and Lewis). In contrast, HR 8799bcd, Fomalhaut b, and β Pictoris b have (to first order) uniformly warm photospheres dominated by internal heat rather than reprocessed host star light. These planets are still young (<300 Myr); like brown dwarfs, their atmospheres will eventually cool to low temperatures.

2.2. Photospheric Pressures

While the mean photospheric gas temperatures of brown dwarfs and planets are comparable, gas pressures are generally quite different. At the photosphere, gas pressure is proportional to the surface gravity, g, as $P_{ph} \propto g/\kappa$, where κ is the Rosseland mean opacity. Evolutionary models dictate that the surface gravities of brown dwarfs depend strongly on mass (due to their nearly constant radii)

and weakly on age (significant variations only for ages $\lesssim 100$ Myr; see Figure 2). Surface gravities for evolved M, L and T dwarfs (ages ~ 0.5 –10 Gyr) span g ~ 300 –3000 m s $^{-2}$. In contrast, the vast majority of transiting exoplanets have g ~ 10 –30 m s $^{-2}$, as directly inferred from radial velocity and transit light curves (e.g., Sozzetti et al. 2007). Ignoring opacity effects, the photospheric gas pressures of transiting exoplanets are 1–2 orders of magnitude less than those of brown dwarfs. Cooler, widely-orbiting Jupiter-mass gas giants also have photospheric pressures about 10 times less than their (typically more massive) brown dwarf counterparts.

Differences in photospheric gas pressure can have a measurable influence on some chemical pathways. One example is the reduction reaction ${\rm CO}+3{\rm H}_2\to {\rm CH}_4+{\rm H}_2{\rm O}$, which favors ${\rm CH}_4$ production in high-pressure gas environments. Chemical equilibrium models indicate that ${\rm CH}_4$ becomes abundant in brown dwarf photospheres (1-10 bar) below $\sim\!1400$ K, but in planetary photospheres (0.01–1 bar) below $\sim\!900$ K (e.g., Lodders & Fegley 2006). Pressure also modulates some gas opacities, notably the pressure-broadened alkali lines that dominate the optical spectra of L and T dwarfs, and collision-induced ${\rm H}_2$ absorption that suppresses broad swaths of infrared light in the coldest brown dwarfs (e.g., Linsky 1969; Saumon et al. 1994). Both features are used to constrain surface gravities for individual brown dwarfs near the Sun (e.g., Martín et al. 1999; Burgasser et al. 2006; Kirkpatrick et al. 2006) and verify the membership of brown dwarfs in young clusters (e.g., Luhman 1999; Allers et al. 2007).

Fortuitously, there is overlap in photospheric gas pressure/temperature space between the youngest and lowest-mass brown dwarfs—those found in young star-forming regions and associations—and dense gas giant planets that are either very massive or have a substantial core. Transiting planets such as HD 147506b (aka Hat-P-2b; $\rho \approx 13$ g cm⁻³; Bakos et al. 2007) and CoRoT-Exo-3b ($\rho \approx 26$ g cm⁻³; Deleuil et al. 2008) have surface gravities similar to 30–100 Myr, ~5–20 Jupiter mass brown dwarfs like 2MASS 1207-39B and AB Pic B (Chauvin et al. 2004, 2005; Mohanty et al. 2007; see Figure 2). With a mass of 22 Jupiter masses, CoRoT-Exo-3b could be properly classified as a highly irradiated brown dwarf companion.

In addition to mean values of photospheric temperature and pressure, differences in the pressure-temperature profiles of brown dwarfs and exoplanets must be considered. For planets, external heating from the host star flattens out the pressure-temperature profile and can give rise to inversion layers. This translates into variations in the local gas chemistry and changes in the atmospheric column abundances of atomic and molecular absorbers. In addition, strongly irradiated planets develop deep radiative envelopes that extend well below the visible photosphere, whereas brown dwarf atmospheres are fully convective through to their photospheres (e.g., Burrows et al. 1997). Differences in the gas mixing rates and vertical temperature profiles between externally heated planetary atmospheres and brown dwarf atmospheres can produce profound differences in emergent spectral energy distributions, even for sources with comparable photospheric gas temperatures and pressures (e.g., Fortney et al. 2008a).

2.3. Compositions

The elemental composition, or metallicity, of a cool atmosphere also modulates chemistry and spectral appearance. Gas-giant planets tend to have metalrich atmospheres, having condensed out of the gas-depleted debris disks around preferentially metal-enriched host stars (e.g., Gonzalez 1997). Ice-giant (i.e., Neptune) and terrestrial planet atmospheres exhibit even greater metallicity enhancements. These trends are present in the solar system: the atmospheres of Jupiter, Saturn, Uranus and Neptune have effective metal abundances ranging from ~3 to ~40 times that of the Sun (Fortney 2007). More importantly, there is a large range in individual elemental abundances, driven by the segregation of volatiles in the Sun's early protoplanetary disk and chemical separation in planetary atmospheres (e.g., He settling in Saturn). Significant variations in elemental abundances can have as great or greater impact on the chemistry and molecular composition of cool atmospheres as pressure or temperature alone (e.g., Tinetti et al. 2007; Fortney et al. 2008b).

In contrast, brown dwarf metallicites are expected to span the same range as stars, topping out at perhaps 3–5 times solar abundances but extending down to significantly subsolar abundances in the metal-poor thick disk and halo populations. For example, members of the recently-identified L subdwarf class have metallicities ~ 0.01 -0.1 times solar (Burgasser et al. 2007; Schilbach et al. 2008). Even brown dwarfs with bulk solar metallicities will have slightly metal-poor photospheres due to condensation effects. Like stars, relative elemental abundances of brown dwarfs are likely to exhibit only small variations, although condensation effects may modify abundance patterns. In any case, the broad range of elemental abundances observed in the solar planets and expected to a greater degree among the wider exoplanet population will probably not be realized among Galactic brown dwarfs.

2.4. Stellar Hosts and Driving Forces

Unlike the majority of brown dwarfs, exoplanets are generally accompanied by a luminous host star, which ultimately maintains its atmosphere in a warm state, modulo variations arising from orbital eccentricity, circulation, or magnetic interaction effects. Radiation and stellar winds drive non-equilibrium dynamics in exoplanet atmospheres, including internal winds/jets (see contribution by Showman) and atmospheric stripping (see contribution by Alyward). UV and X-ray radiation drive photochemical production of hazes in exoplanet atmospheres (see contribution by Yung), and the formation of upper inversion layers. Tidal locking from a close stellar companion slows an exoplanet's rotation and can provide a source of (temporary) internal heating.

These processes will not generally occur in brown dwarf atmospheres. The hottest and youngest brown dwarfs do exhibit high-energy nonthermal emission (X-ray and UV) arising from magnetic activity or accretion. However, with the exception of rare massive flares in which the total magnetic energy output can briefly exceed thermal emission (e.g., Liebert et al. 1999), high-energy magnetic emission is typically a small fraction ($<10^{-3}$) of the total energy budget and does not significantly alter pressure-temperature profiles. Furthermore, for cooler L and T-type brown dwarfs, magnetic emission is conspicuously absent due to the loss of field/gas coupling in the highly neutral photospheres of these objects

(Mohanty et al. 2002; Gelino et al. 2002). Only the very youngest (<1 Myr), actively accreting brown dwarfs and sources in close orbits around luminous companions are likely to show significant modification of their pressure-temperature profiles as a result of external driving forces.

The absence of both radiative and mechanical forcing on brown dwarf atmospheres is particularly relevant to atmospheric circulation and dynamics (see contributions by Showman and Cho). Rotational modulation of weather phenomena has been invoked to explain low-level spectral and photometric variability detected in some brown dwarfs (see review by Goldman 2005). The timescales for these variations are generally consistent with rotational line broadening measurements (e.g., Reiners & Basri 2008) and variations in nonthermal magnetic emission (e.g., Berger 2006). The general absence of magnetic field coupling (i.e., spots) and the clear presence of condensate clouds makes weather an appealing explanation for this variability, particularly given observed longterm period variations and changes in variability amplitudes. However, the winds and jets that drive weather in planetary atmospheres arise from asymmetric radiative forcing by the host star; such forces are absent for most brown dwarfs. It is possible that winds could be driven by the extremely rapid rotations of brown dwarfs. Periods of 1–10 hours are typical (cf. Jupiter's 11-hour period) and surface rotational velocities of up to 80 km s⁻¹ have been measured (Reiners & Basri 2008). This is an order of magnitude faster than the rotations of tidally-locked giant planets, and as a result coriolis forcing is more important in brown dwarf atmospheres. However, because of their greater surface gravities and photospheric pressures, the Rhines length and Rossby deformation radius scales (see contribution by Showman) in the upper atmospheres of brown dwarfs are roughly equivalent to those for hot Jupiters, of order the planetary/brown dwarf radius (assuming horizontal wind speeds comparable to the local sound speed, $\sim 1 \text{ km s}^{-1}$; see Showman et al. 2008). As such, the small-scale banding and storm vorticities that characterize Jupiter's visible atmosphere are probably not common on either brown dwarfs or hot Jupiters, although detailed modeling of the former have yet to be reported.

In summary, while the current populations of brown dwarfs and (warm/hot) exoplanets may have photospheres with similar temperatures, significant differences in gas pressures and compositions may drive markedly dissimilar molecular chemistry. There is some overlap in temperature/pressure space between the densest/most massive exoplanets and the youngest/least-massive brown dwarfs, where meaningful comparisons in atmospheric properties and processes may be fruitfully made. The external forcing of a host star also results in exoplanetary atmospheric processes not seen in brown dwarfs: modified pressure-temperature profiles, inversion layers, photochemical production and thermal asymmetries that drive winds and jets. Yet at least in terms of flow dynamics, the atmospheres of both tidally-locked hot Jupiters and brown dwarfs should be weakly banded and have few small-scale vorticities in contrast to Jupiter.

3. Detailed Brown Dwarf Results Relevant to Exoplanet Studies

I conclude my contribution with two examples of low-temperature atmospheric processes studied in detail in brown dwarf studies but not yet sufficiently con-

strained in exoplanetary studies: condensate cloud formation and nonequilibrium chemistry.

3.1. Condensate Cloud Formation

Condensed species present in the photospheres of L dwarfs arise naturally from equilibrium chemistry, proceeding from the more refractory species such as mineral oxides and silicates (below 2500 K), to ionic salts and sulfides (below 1000 K), to "organic" condensates including as $H_2O[s]$ and $NH_3[s]$ (below 300 K; see review by Lodders & Fegley 2006). The presence of condensed species in L dwarfs has been inferred indirectly by their very red colors and muted molecular absorption features (e.g., Allard et al. 2001). Direct detection of silicate grain absorption has recently been made possible by the *Spitzer Space Telescope* (Cushing et al. 2006).

That these species reside in cloud structures in brown dwarf atmospheres has be inferred from other indicators: elemental depletion at high altitudes and the absence of condensates in T dwarf spectra. In the first case, the gravitational settling of condensed grains removes these species from the ambient gas, preventing further chemical reactions at higher (cooler) altitudes. For example, K I absorption is particularly strong in T dwarf spectra, despite the fact that K should have condensed out into silicate grains such as KAlSi₃O₈[s] (othroclase). This reaction is inhibited by the depletion of Al and Si at deeper layers through the formation of, e.g., CaTiO₃[s] (perovskite) and Al₂O₃[s] (corundum; Burrows & Sharp 1999; Lodders & Fegley 2006); hence elemental K persists.³ The absence of condensate cloud absorption in T dwarf spectra can be explained if condensates are vertically confined in cloud structures which ultimately sink below the visible photosphere (e.g., Ackerman & Marley 2001; Tsuji 2002; Cooper et al. 2003; Woitke & Helling 2004). As it turns out, the disappearance of condensate clouds at the transition between L and T dwarfs is quite abrupt, suggesting dynamic effects may be critical for cloud evolution (e.g., Burgasser et al. 2002; Liu et al. 2006; Burgasser 2007; Cushing et al. 2008).

The >500 L dwarfs observed to date reveal substantial diversity in cloudsensitive features, including near-infrared colors (>1 mag scatter in J-K for a given spectral subtype) and the strength of silicate grain absorption (e.g., Kirkpatrick et al. 2000; McLean et al. 2003; Burgasser et al. 2008). These variations have been simplistically interrupted as a range in cloud "thicknesses" (e.g. Cushing et al. 2008), although it is likely that other properties, such as grain size distribution, grain compositions (e.g., Helling et al. 2008) and cloud surface coverage also contribute. The properties of brown dwarf clouds are almost certainly tied to (interrelated) secondary parameters of age, surface gravity, metallicity, and rotation, as suggested by empirical trends (e.g., Faherty et al. 2009). However, current atmospheric models generally treat cloud properties as an independent model parameter, so source-to-source variations and temporal evolution can only be treated in a somewhat ad-hoc manner. Nevertheless, there has been substantial improvement in the fidelty and complexity of con-

 $^{^3}$ Condensate depletion is also seen in the atmospheres of Jupiter and Saturn as traced by the presence of $GeH_4[s]$ (germane) over $SiH_4[s]$ (silane), despite the much greater elemental abundance of Si in a solar gas mixture (Fegley & Lodders 1994).

densate cloud models to address the wealth of observational data, progress that can be ported to the still underconstrained problem of condensate clouds in hot exoplanetary atmospheres.

3.2. Nonequilibrium Chemistry and Atmospheric Dynamics

The contribution of Marley touches upon nonequilibrium chemistry in brown dwarf atmospheres in considerable detail, so I present only the major results here for completeness. Nonequilibrium chemistry refers to the nonequilibrium abundances of species that occur when the timescale for diffusive gas flow is shorter than the timescales governing the relevant chemical reactions. In brown dwarfs, the two reactions that are most affected by nonequilibrium chemistry convert $CO \rightarrow CH_4$ and $N_2 \rightarrow NH_3$. CO and N_2 have strong bonds and long chemical timescales at low temperatures, so they can appear in excess, and CH₄ and NH₃ in depletion, as a result of diffusive flows. Such abundance anomalies are indeed observed (Noll et al. 1997; Oppenheimer et al. 1998; Saumon et al. 2006), and indicate diffusivity constants of 1-100 m² s⁻¹, in excess of flows expected from convective instabilities (Saumon et al. 2007). It is likely that nonequilbrium chemistry is present in exoplanetary atmospheres as well, potentially giving rise to azimuthal abundance variations in sources with large day/night asymmetries, and hence modulation of phase-resolved spectroscopy in variance with equilibrium chemistry models. Such effects should be specifically sought for in future phase-resolved, direct spectroscopic studies of transiting exoplanets.

Acknowledgments. I thank A. Showman for insightful conversations on planetary atmospheric flow scales, K. Lodders and M. Marley for consultation on theoretical topics, and M. Cushing for providing Figure 1.

References

Ackerman, A. S., & Marley, M. S. 2001, ApJ, 556, 872

Allard, F., Hauschildt, P. H., Alexander, D. R., Tamanai, A., & Schweitzer, A. 2001, ApJ, 556, 357

Allard, N. F., Allard, F., Hauschildt, P. H., Kielkopf, J. F., & Machin, L. 2003, A&A, 411, L473

Allers, K. N., et al. 2007, ApJ, 657, 511

Bakos, G. Á., et al. 2007, ApJ, 670, 826

Barber, R. J., Tennyson, J., Harris, G. J., & Tolchenov, R. N. 2006, MNRAS, 368, 1087 Basri, G., & Brown, M. E. 2006, Annual Review of Earth and Planetary Sciences, 34, 193

Berger, E. 2006, ApJ, 648, 629

Burgasser, A. J. 2007, ApJ, 659, 655

Burgasser, A. J., Burrows, A., & Kirkpatrick, J. D. 2006, ApJ, 639, 1095

Burgasser, A. J., Cruz, K. L., & Kirkpatrick, J. D. 2007, ApJ, 657, 494

Burgasser, A. J., Looper, D. L., Kirkpatrick, J. D., Cruz, K. L., & Swift, B. J. 2008, ApJ, 674, 451

Burgasser, A. J., Marley, M. S., Ackerman, A. S., Saumon, D., Lodders, K., Dahn, C. C., Harris, H. C., & Kirkpatrick, J. D. 2002, ApJ, 571, L151

Burningham, B., et al. 2008, MNRAS, 391, 320

Burrows, A., Hubbard, W. B., Lunine, J. I., & Liebert, J. 2001, Reviews of Modern Physics, 73, 719

Burrows, A., Marley, M., Hubbard, W. B., Lunine, J. I., Guillot, T., Saumon, D., Freedman, R., Sudarsky, D., & Sharp, C. 1997, ApJ, 491, 856

Burrows, A., & Sharp, C. M. 1999, ApJ, 512, 843

Burrows, A., & Volobuyev, M. 2003, ApJ, 583, 985

Chabrier, G., & Baraffe, I. 2000, ARA&A, 38, 337

Chauvin, G., Lagrange, A.-M., Dumas, C., Zuckerman, B., Mouillet, D., Song, I., Beuzit, J.-L., & Lowrance, P. 2004, A&A, 425, L29

Chauvin, G., Lagrange, A.-M., Zuckerman, B., Dumas, C., Mouillet, D., Song, I., Beuzit, J.-L., Lowrance, P., & Bessell, M. S. 2005, A&A, 438, L29

Cooper, C. S., Sudarsky, D., Milsom, J. A., Lunine, J. I., & Burrows, A. 2003, ApJ, 586, 1320

Cushing, M. C., Marley, M. S., Saumon, D., Kelly, B. C., Vacca, W. D., Rayner, J. T., Freedman, R. S., Lodders, K., & Roellig, T. L. 2008, ApJ, 678, 1372

Cushing, M. C., et al. 2006, ApJ, 648, 614

Dahn, C. C., et al. 2002, AJ, 124, 1170

Deleuil, M., et al. 2008, A&A, 491, 889

Delorme, P., et al. 2008, A&A, 482, 961

Dupuy, T. J., Liu, M. C., & Ireland, M. J. 2008, ArXiv e-prints

Faherty, J. K., Burgasser, A. J., Cruz, K. L., Shara, M. M., Walter, F. M., & Gelino, C. R. 2009, AJ, 137, 1

Fegley, B. J., & Lodders, K. 1994, Icarus, 110, 117

Fortney, J. J. 2007, Ap&SS, 307, 279

Fortney, J. J., Lodders, K., Marley, M. S., & Freedman, R. S. 2008a, ApJ, 678, 1419

Fortney, J. J., Marley, M. S., Saumon, D., & Lodders, K. 2008b, ApJ, 683, 1104

Freedman, R. S., Marley, M. S., & Lodders, K. 2008, ApJS, 174, 504

Gelino, C. R., Marley, M. S., Holtzman, J. A., Ackerman, A. S., & Lodders, K. 2002, ApJ, 577, 433

Goldman, B. 2005, Astronomische Nachrichten, 326, 1059

Golimowski, D. A., et al. 2004, AJ, 127, 3516

Gonzalez, G. 1997, MNRAS, 285, 403

Griffith, C. A., & Yelle, R. V. 1999, ApJ, 519, L85

Helling, C., Dehn, M., Woitke, P., & Hauschildt, P. H. 2008, ApJ, 675, L105

Helling, C., & Woitke, P. 2006, A&A, 455, 325

Kalas, P., Graham, J. R., Chiang, E., Fitzgerald, M. P., Clampin, M., Kite, E. S., Stapelfeldt, K., Marois, C., & Krist, J. 2008, Science, 322, 1345

Kirkpatrick, J. D. 2005, ARA&A, 43, 195

Kirkpatrick, J. D., Barman, T. S., Burgasser, A. J., McGovern, M. R., McLean, I. S., Tinney, C. G., & Lowrance, P. J. 2006, ApJ, 639, 1120

Kirkpatrick, J. D., Dahn, C. C., Monet, D. G., Reid, I. N., Gizis, J. E., Liebert, J., & Burgasser, A. J. 2001, AJ, 121, 3235

Kirkpatrick, J. D., Reid, I. N., Liebert, J., Gizis, J. E., Burgasser, A. J., Monet, D. G., Dahn, C. C., Nelson, B., & Williams, R. J. 2000, AJ, 120, 447

Kunde, V. G., et al. 2004, Science, 305, 1582

Lagrange, A., et al. 2008, ArXiv e-prints

Leggett, S. K., Saumon, D., Albert, L., Cushing, M. C., Liu, M. C., Luhman, K. L., Marley, M. S., Kirkpatrick, J. D., Roellig, T. L., & Allers, K. N. 2008, ApJ, 682, 1256

Liebert, J., Kirkpatrick, J. D., Reid, I. N., & Fisher, M. D. 1999, ApJ, 519, 345

Linsky, J. L. 1969, ApJ, 156, 989

Liu, M. C., Leggett, S. K., Golimowski, D. A., Chiu, K., Fan, X., Geballe, T. R., Schneider, D. P., & Brinkmann, J. 2006, ApJ, 647, 1393

Lodders, K., & Fegley, Jr., B. 2006, Chemistry of Low Mass Substellar Objects (Astrophysics Update 2), 1–+

Luhman, K. L. 1999, ApJ, 525, 466

Luhman, K. L., Joergens, V., Lada, C., Muzerolle, J., Pascucci, I., & White, R. 2007, Protostars and Planets V, 443

Marois, C., Macintosh, B., Barman, T., Zuckerman, B., Song, I., Patience, J., Lafreniere,

D., & Doyon, R. 2008, ArXiv e-prints

Marley, M. S., & Leggett, S. K. 2008, in The Future of Ultracool Dwarf Science with JWST, ArXiv e-prints 0803.1476

Martín, E. L., Delfosse, X., Basri, G., Goldman, B., Forveille, T., & Zapatero Osorio, M. R. 1999, AJ, 118, 2466

Mayor, M., & Queloz, D. 1995, Nat, 378, 355

McLean, I. S., McGovern, M. R., Burgasser, A. J., Kirkpatrick, J. D., Prato, L., & Kim, S. S. 2003, ApJ, 596, 561

Metchev, S. A., & Hillenbrand, L. A. 2006, ApJ, 651, 1166

Mohanty, S., Basri, G., Jayawardhana, R., Allard, F., Hauschildt, P., & Ardila, D. 2004a, ApJ, 609, 854

Mohanty, S., Basri, G., Shu, F., Allard, F., & Chabrier, G. 2002, ApJ, 571, 469

Mohanty, S., Jayawardhana, R., & Basri, G. 2004b, ApJ, 609, 885

Mohanty, S., Jayawardhana, R., Huélamo, N., & Mamajek, E. 2007, ApJ, 657, 1064

Nakajima, T., Oppenheimer, B. R., Kulkarni, S. R., Golimowski, D. A., Matthews, K., & Durrance, S. T. 1995, Nat, 378, 463

Noll, K. S., Geballe, T. R., & Marley, M. S. 1997, ApJ, 489, L87+

Oppenheimer, B. R., Kulkarni, S. R., Matthews, K., & van Kerkwijk, M. H. 1998, ApJ, 502, 932

Oppenheimer, B. R., Kulkarni, S. R., & Stauffer, J. R. 2000, Protostars and Planets IV, 1313

Rayner, J. T., Cushing, M. C., & Vacca, W. D. 2009, in preparation

Reiners, A., & Basri, G. 2008, ApJ, 684, 1390

Saumon, D., Bergeron, P., Lunine, J. I., Hubbard, W. B., & Burrows, A. 1994, ApJ, 424, 333

Saumon, D., Marley, M. S., Cushing, M. C., Leggett, S. K., Roellig, T. L., Lodders, K., & Freedman, R. S. 2006, ApJ, 647, 552

Saumon, D., et al. 2007, ApJ, 656, 552

Schilbach, E., Roeser, S., & Scholz, R. . 2008, ArXiv e-prints

Showman, A. P., Menou, K., & Cho, J. Y.-K. 2008, in Astronomical Society of the Pacific Conference Series, Vol. 398, Astronomical Society of the Pacific Conference Series, ed. D. Fischer, F. A. Rasio, S. E. Thorsett, & A. Wolszczan, 419–+

Smith, V. V., Tsuji, T., Hinkle, K. H., Cunha, K., Blum, R. D., Valenti, J. A., Ridgway, S. T., Joyce, R. R., & Bernath, P. 2003, ApJ, 599, L107

Sozzetti, A., Torres, G., Charbonneau, D., Latham, D. W., Holman, M. J., Winn, J. N., Laird, J. B., & O'Donovan, F. T. 2007, ApJ, 664, 1190

Tinetti, G., Liang, M.-C., Vidal-Madjar, A., Ehrenreich, D., Lecavelier des Etangs, A., & Yung, Y. L. 2007, ApJ, 654, L99

Torres, G., Winn, J. N., & Holman, M. J. 2008, ApJ, 677, 1324

Tsuji, T. 2002, ApJ, 575, 264

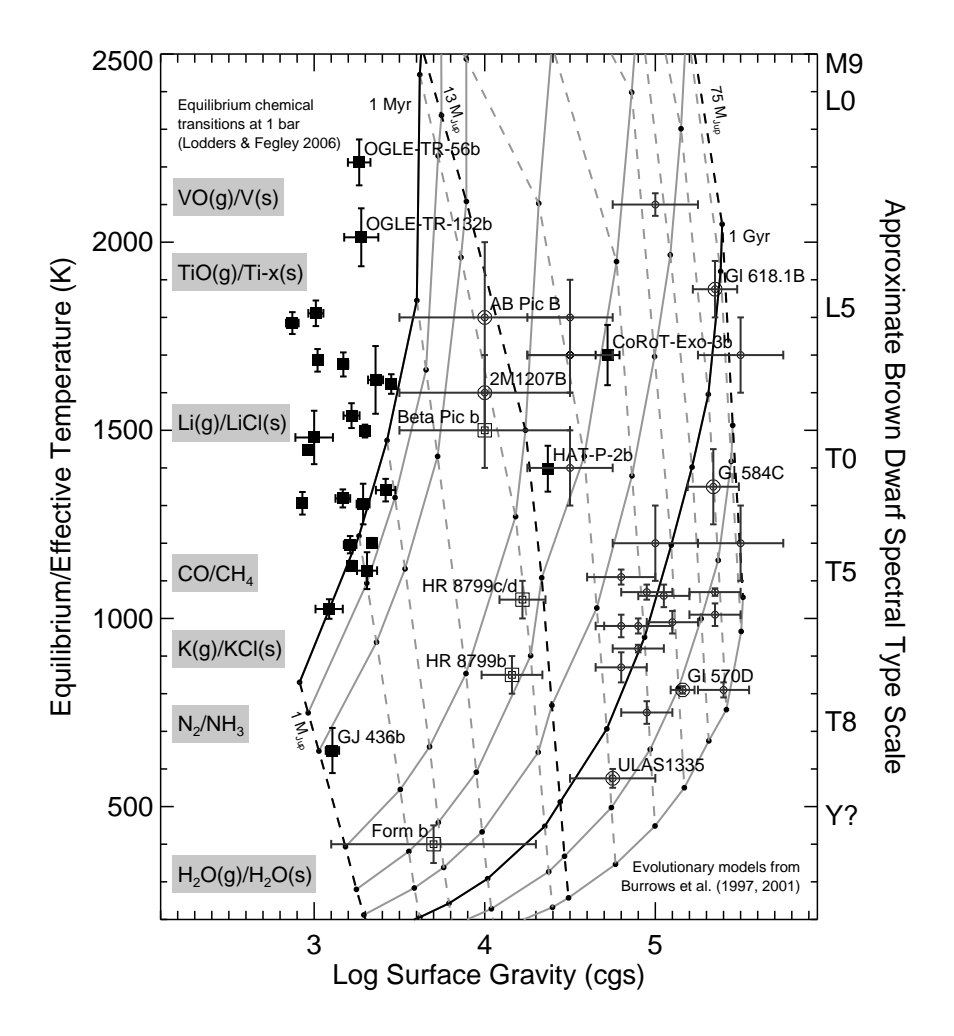
Vrba, F. J., et al. 2004, AJ, 127, 2948

Whitworth, A., Bate, M. R., Nordlund, Å., Reipurth, B., & Zinnecker, H. 2007, Protostars and Planets V, 459

Wilson, J. C., Kirkpatrick, J. D., Gizis, J. E., Skrutskie, M. F., Monet, D. G., & Houck, J. R. 2001, AJ, 122, 1989

Woitke, P., & Helling, C. 2004, A&A, 414, 335

Zapatero Osorio, M. R., Lane, B. F., Pavlenko, Y., Martín, E. L., Britton, M., & Kulkarni, S. R. 2004, ApJ, 615, 958



Atmospheric gas properties of extrasolar planets and brown dwarfs, as traced by T_{eff}/T_{eq} and surface gravity. T_{eq} and g values for transiting planets are from Torres et al. (2008) and indicated by solid black squares (outliers are specifically labeled). Inferred T_{eff} and g parameters for the directly detected planets, HR 8799bcd (Marois et al. 2008), Fomalhaut b (Kalas et al. 2008), and β Pictoris b (Lagrange et al. 2008) are indicated by open squares and labeled. T_{eff} and g parameters for several field brown dwarfs (Burgasser et al. 2006; Cushing et al. 2008) and a sample of benchmark sources (labelled; Mohanty et al. 2007; Kirkpatrick et al. 2001; Wilson et al. 2001; Saumon et al. 2006; Chauvin et al. 2005; Burningham et al. 2008) are indicated by open circles. These measurements are compared to the brown dwarf ("hot start") evolutionary models of Burrows et al. (1997, 2001). Solid lines delineate ages of 1, 5, 10, 30, 100, 300 Myr and 1, 3, and 10 Gyr, with 1 Myr and 1 Gyr isochrones highlighted. Dashed lines delineate masses of 0.001, 0.002, 0.003, 0.005, 0.01, 0.012, 0.02, 0.03, 0.04, 0.05, 0.06, 0.07 and $0.072 M_{\odot}$, with the $0.001~\mathrm{M}_{\odot} = 1~\mathrm{Jupiter~mass},\, 0.012~\mathrm{M}_{\odot} = 13~\mathrm{Jupiter~masses}$ (deuterium burning limit) and $0.072 \text{ M}_{\odot} = 75 \text{ Jupiter masses (hydrogen burning limit) lines}$ highlighted. An approximate spectral classification scale based on T_{eff} determinations by Vrba et al. (2004) is indicated on the right axis. Equilibrium chemical transitions for several key species are indicated along the left side of the plot (Lodders & Fegley 2006).